

Availability of Aerial Heterogeneous Networks for Reliable Emergency Communications

Teng Wu^{†‡}, Jiandong Li[†], Junyu Liu[†], Min Sheng[†], Mohammadali Mohammadi[‡], Hien Quoc Ngo[‡], and Michail Matthaiou[‡]

[†]State Key Laboratory of ISN, Institute of Information Science, Xidian University, Xi'an, Shaanxi, 710071, China

[‡]Centre for Wireless Innovation (CWI), Queen's University Belfast, Belfast, BT3 9DT, United Kingdom

Email: t.wu@stu.xidian.edu.cn

Abstract—We investigate network availability (NA) in aerial heterogeneous networks (AHetNets) for effective emergency rescue, where diverse delay-constrained communication services must be provided to user equipments (UEs) with varying mobility. The heterogeneity in delay constraints and UE mobility introduces resource allocation conflicts and imbalances, which undermine communication reliability and challenge NA. Although unified resource allocation (URA) can mitigate these issues, it remains unclear whether NA can be sustained under such diverse conditions. To address this, we derive expressions for the lower bound (LB) on NA in AHetNets under URA. Our analysis reveals that extended heterogeneity significantly degrades the LB due to resource limitations—even when the heterogeneity stems from additional services under less stringent delay constraints (LSDC) or from UEs with lower mobility. To overcome this degradation, we formulate and solve a joint optimization problem for the number of UEs sharing time-frequency resources (K) and pilot length (ξ), aiming to enhance the LB by improving spatial, frequency, and temporal resource efficiency. Simulation results validate our analysis and demonstrate that jointly optimizing K and ξ enables AHetNets to achieve the target NA under greater heterogeneity, outperforming existing resource allocation policies.

Index Terms—Aerial heterogeneous network, diverse delay constraints, diverse mobility, reliable emergency communication.

I. INTRODUCTION

Providing emergency communications to counteract the detrimental effects of physical disasters is a key use case of sixth-generation (6G) globalization [1]. Benefiting from flexibility and adaptability, unmanned aerial vehicle (UAV) communications are particularly suitable for emergencies [2]. On one hand, UAVs equipped with thermal imagers, infrared scanners, and cameras as aerial UEs (AUEs) can collect vital information for search and rescue. On the other hand, aerial networks with UAV-mounted flying access points (FAPs) can be swiftly deployed for providing emergency communications to AUEs and ground UEs (GUEs) of rescuers and survivors.

Despite their potential, emergency communication services for disaster rescue face formidable challenges. Unreliability arises from dynamic channels due to FAP movement, wireless fading, and service burstiness [3], [4]. Additionally, AUEs and

This work is supported in part by Natural Science Foundation of China (Grant No. 62121001), in part by Key Research and Development Program of Shanxi (Grant No. 2024CY2-GJHX-82), and in part by China Scholarship Council (Student ID: 202506960051). The work of M. Matthaiou was supported by the European Research Council (ERC) under the European Union's Horizon 2020 research and innovation programme (grant agreement No. 101001331).

GUEs exhibit distinct mobility and require communications under diverse delay constraints—from second-level delays for real-time media to sub-millisecond delays for remote control [2]. This heterogeneity causes resource allocation conflicts and imbalances [3], undermining reliability. As a result, the NA of AHetNets is hindered from supporting effective emergency rescue, where NA is the probability that the quality-of-service (QoS) requirements, in terms of delay and reliability, for each UE's service are satisfied [4].

Recent works suggest that coordinated multi-point (CoMP) can address unreliability from dynamic channels, wireless fading, and service burstiness, even when AUEs and GUEs coexist [4]–[6]. Effective resource allocation under CoMP for diverse delay constraints [7] and UE mobility [8] can enhance transmission rates and reliability. However, existing works largely overlook how delay constraints and UE mobility jointly affect NA. Most studies focus on a single delay constraint or UE mobility type [4], and although URA appears suitable for heterogeneous networks [9], its viability under diverse delay and mobility remains unclear. Consequently, NA in AHetNets is not yet well understood, and current resource allocation strategies cannot be directly applied to achieve the target NA.

Motivated by the above, this work investigates the NA of FAP CoMP-enabled AHetNets for reliable emergency communication (REC) services under a URA scheme. The main contributions of this paper are as follows:

- We derive a LB on NA for performance analysis and show that it is significantly degraded under extended heterogeneity due to reduced resources in URA, even when heterogeneity stems from additional REC services under LSDC or from UEs with lower mobility.
- Our analysis reveals that jointly optimizing the number of UEs sharing time-frequency resources (K) and pilot length (ξ) can effectively improve spatial, frequency, and temporal resource efficiency, thereby enhancing the LB on NA. Building on this insight, we formulate and solve a joint optimization problem for K and ξ to enhance NA.
- Our simulation results confirm that the target NA is achievable even under greater heterogeneity by jointly optimizing K and ξ , outperforming existing policies.

Notations: $\mathbb{E}_X[\cdot]$ denotes the expectation with respect to (w.r.t.) the random variable (RV) X ; $\mathbb{P}_X(\cdot)$ denotes the probability w.r.t. the RV X ; $\lfloor \cdot \rfloor$ and $\lceil \cdot \rceil$ are the floor and ceil opera-

tors, respectively; $\mathbb{1}[Y]$ denotes the indicator function of event Y , where $\mathbb{1}[Y] = 1$ if event Y is true, and $\mathbb{1}[Y] = 0$ otherwise; $z \sim \mathcal{CN}(0, \sigma^2)$ denotes a complex Gaussian RV z with zero mean and variance σ^2 ; $f_{Q^{-1}}(\cdot)$ is the inverse Q-function, while the Q-function is $f_Q(x) = \frac{1}{\sqrt{2\pi}} \int_x^\infty \exp(-\frac{y^2}{2}) dy$. Finally, $J_0(\cdot)$ is the zeroth-order Bessel function of the first kind.

II. SYSTEM MODEL

A. Network Model

We consider an uplink FAP CoMP-enabled AHetNet, which consists of L fixed-wing UAV-mounted single-antenna FAPs and M single-antenna UEs with diverse mobility. In general, $M \gg L$. All FAPs are connected to a central processor (CP) via wireless fronthaul links for centralized signal processing, while the CP can be deployed on the ground or in the sky [4]. We consider that the disaster occurs in a circular area with a radius W_D , which is denoted as the disaster area \mathcal{A} . The UEs include AUEs and GUEs, where GUEs are randomly distributed within \mathcal{A} , while AUEs are randomly distributed over the altitude range $\mathcal{H} = [h_{\min}, h_{\max}]$ above \mathcal{A} . Moreover, h_{\min} and h_{\max} are the minimum and maximum altitudes where AUEs are located, respectively. All FAPs follow periodic circular flight trajectories. The flight altitude, radius, and velocity of each FAP are h_F , W_F , and v_F , respectively. Thus, the flight period of each FAP is $T = 2\pi W_F / v_F$. We equally divide T into I time slots with a duration T_S , while T_S is generally chosen as a value less than the coherence interval T_C , i.e., $I = T / T_S$, $t = iT_S$, $\forall t \in [0, T]$, $\forall i \in [0, I]$, and $T_S \leq T_C$. The UE mobility in AHetNets is characterized by the relative velocity v_r between UEs and FAPs. We consider that all FAPs have the same v_r w.r.t. the same UE, while v_r may vary across different UEs due to diverse mobility. Moreover, we consider that each transmission distance from UEs to FAPs $d = \sqrt{d_H^2 + h^2}$ is constant during one time slot and varies between different time slots [4], where d_H and h are the horizontal and vertical distances from UEs to FAPs, respectively. The farthest transmission distance from UEs to FAPs is $\tilde{d} = \sqrt{\tilde{d}_H^2 + \tilde{h}^2}$, where $\tilde{d}_H = 2W_D + 2W_F$ and $\tilde{h} = \max\{h_F, |h_F - h_{\min}|, |h_F - h_{\max}|\}$ are the farthest horizontal and vertical distances from UEs to FAPs, respectively.

B. Traffic Model and Scheduling

In general, RECs are delay-sensitive services with burstiness, where delay constraints primarily include LSDC and more stringent delay constraints (MSDC) categories [2], [3], [10]. The service burstiness can be characterized by the variance of the random arrival rates [3]. Thus, the arrival processes of REC services are modeled as stochastic arrival processes with average arrival rate θ^ς and arrival rate variance σ_ς^2 , $\varsigma \in \{\text{LS}, \text{MS}\}$, where LS and MS denote REC services under LSDC and MSDC, respectively. To manage unreliability due to bursty services, we consider deploying a first-come-first-serve server in the system for uplink traffic scheduling, which is a common and effective method [3], [4]. As a result, there will be a queue at the buffer in the UE.

C. Channel Model

We consider both quasi-static and time-varying channels due to diverse delay constraints and UE mobility [4], [11].

1) *Quasi-Static Channel*: The channels from UEs to FAPs are independent identically distributed (i.i.d.) during different coherence intervals and can be modeled as [4]

$$g = \sqrt{\beta}\psi, \quad (1)$$

where ψ denotes the small-scale and shadow fading that is modeled as κ - μ shadowed fading; β denotes the path loss that is assumed to be known a priori and modeled as $\beta(d) = Ad^{-2}$; \mathcal{A} (dB) = $-20\log_{10}(4\pi/\lambda)$ denotes the path loss at 1 m with wavelength $\lambda = v_L/f_c$; f_c is the carrier frequency, while v_L is the speed of light.

2) *Time-Varying Channel*: The channels from UEs to FAPs between adjacent coherence intervals are correlated. We apply a first-order auto-regressive (AR) model to portray the channel correlation [11]. In that, the channels can be modeled as

$$g = e_c g_{-1} + \sqrt{1 - e_c^2} e_{\text{unc}}, \quad (2)$$

where $e_{\text{unc}} \sim \mathcal{CN}(0, \beta)$ denotes the innovation component during one coherence interval that is uncorrelated with the channel during the previous coherence interval g_{-1} ; e_c is the temporal correlation coefficient between adjacent coherence intervals that can be calculated by using Jakes fading model. Specifically, $e_c = J_0(2\pi f_D t_s)$, where t_s is the sampling time and $f_D = v_r f_c / v_L$ is the corresponding Doppler frequency shift of v_r between UEs and FAPs. Finally, the coherence interval is $T_C(v_r) \triangleq 9v_L / (16\pi f_c v_r)$ [4]. Note that (2) is applicable for the channels during non-initial coherence intervals of each service, while the channels during the initial coherence interval of each service are modeled as (1).

III. PRELIMINARY ANALYSIS

A. QoS Requirements

For each UE's uplink REC service, the QoS requirements, in terms of delay and reliability, are characterized by the total delay bound in the uplink D_{\max}^ς and the requirement of the uplink overall packet loss (uOPL) probability $\varepsilon_{\max}^\varsigma$ [4]. Thus, the QoS requirements ($D_{\max}^\varsigma, \varepsilon_{\max}^\varsigma$) for each UE's uplink REC service can be satisfied under the following constraints:

$$D^\varsigma \leq D_{\max}^\varsigma, \varepsilon^\varsigma \leq \varepsilon_{\max}^\varsigma, \quad (3)$$

where D^ς is the total delay in the uplink; $\varepsilon^\varsigma = \mathbb{E}_\psi[\varepsilon_\psi^\varsigma]$ is the uOPL probability averaged over the small-scale and shadow fading; $\varepsilon_\psi^\varsigma$ is the uOPL probability under instantaneous fading; $\varsigma \in \{\text{LS}, \text{MS}\}$. Services under both MSDC and LSDC exhibit diverse delay constraints, where D_{\max}^{MS} is sub-millisecond level and D_{\max}^{LS} is millisecond level or higher [10].

According to the 3rd Generation Partnership Project (3GPP) specifications, the total delay in the uplink includes, but is not limited to, the transmission delay, queueing delay, propagation delay, as well as coding and processing delay [12]. This paper focuses on managing spatial, frequency, and temporal resources, which pertain to the transmission delay and queueing delay [3], [4]. Therefore, this paper considers that the total uplink delay D^ς consists of the uplink transmission delay D^u and queueing delay $D^{q,\varsigma}$, i.e., $D^\varsigma = D^u + D^{q,\varsigma}$. To satisfy delay constraints, we employ a short frame structure [3], [4].

The frame duration T_f equals the transmission time interval (TTI), which is the minimal time granularity of the network. Each frame can include data transmission part with duration $T_f^{(d)}$ and control signaling part with duration $T_f^{(c)}$. In this paper, we design the control signaling as orthogonal pilots to estimate channel state information (CSI) [3], [4]. Each uplink transmission takes one frame. The queueing delay is bounded as $D_{\max}^{q,s} \triangleq D_{\max}^s - D^u$.

According to [3], [4], we consider that the transmitted packet will be discarded if any decoding error occurs at the receiver. Moreover, if the queueing delay exceeds its bound, the transmitted packet will be discarded. As a result, the decoding error probability and queueing delay violation probability should be considered in the uOPL probability ε_ψ^s to effectively reflect reliability.

B. Network Availability

The NA is defined as the probability that the QoS requirements, in terms of delay and reliability, for each UE's service are satisfied [4]. Thus, the NA can be expressed as

$$\eta \triangleq \frac{1}{M} \sum_{m=1}^M \mathbb{1}[(D^s \leq D_{\max}^s, \bar{\varepsilon}^s \leq \varepsilon_{\max}^s)_m], \quad (4)$$

where $(D^s \leq D_{\max}^s, \bar{\varepsilon}^s \leq \varepsilon_{\max}^s)_m$ is an event that the delay and reliability requirements for the m th UE's service are satisfied.

Given a target NA η_{\max} , achieving $(\eta \geq \eta_{\max}, \eta_{\max} \rightarrow 1)$ indicates that each UE's REC service is ensured. However, the NA definition in (4) fails to intuitively reveal the impact of heterogeneity that stems from diverse delay constraints and UE mobility. Moreover, the NA evaluation in aerial networks must account for both temporal and spatial dimensions due to FAP movement [4]. Consequently, the NA analysis in AHetNets becomes highly complex. Inspired by [13], we consider a worst-case scenario to explore the LB on NA, where all UEs are activated and each transmission distance from UEs to FAPs is the farthest, i.e., $d = \tilde{d}$. As a result, the NA evaluation for services with identical QoS requirements of UEs with same mobility is simplified because the spatial and temporal dimensions can be omitted, which facilitates the NA analysis in AHetNets. This simplification is articulated in *Lemma 1*.

Lemma 1: The NA for services with identical QoS requirements $(D_{\max}^s, \varepsilon_{\max}^s)$ of UEs with same mobility can be lower bounded by $\mathbb{P}_\psi(D^s \leq D_{\max}^s, \varepsilon_\psi^s \leq \varepsilon_{\max}^s)$ of any UE under the condition that $d = \tilde{d}$.

Proof: The LB on NA is due to the fact that NA will be degraded as d increases [4]. \square

C. URA-based CoMP Packet Delivery Mechanism

In the URA scheme, M UEs are partitioned into K proximity-based clusters, each containing at most $N = \lceil M/K \rceil$ UEs. This strategy is independent of the delay constraints, UE categories, and mobility. The total bandwidth B^{tot} is evenly divided into N orthogonal subchannels, where each UE occupies one subchannel. The per-subchannel bandwidth obeys $B_0 \leq B = N_0 B_0 \leq B_C$ [3], [4], where B_0 is the orthogonal subcarrier spacing, $1 \leq N_0 = \lfloor B^{\text{tot}}/(B_0 N) \rfloor \leq$

$\lfloor B_C/B_0 \rfloor$ is the number of orthogonal subcarriers in each subchannel, while B_C is the coherence bandwidth. Thus, the number of orthogonal subchannels is constrained by

$$N_I = \left\lfloor \frac{B^{\text{tot}}}{B_C} \right\rfloor \leq N \leq N_{II} = \left\lfloor \frac{B^{\text{tot}}}{B_0} \right\rfloor. \quad (5)$$

The UEs within a cluster are interference-free by availing of orthogonal subchannels. Across clusters, UEs sharing time-frequency resources form a UE group whose mutual interference is managed by FAP CoMP. There are N UE groups. Within a group, UEs are referred to as scheduled UEs. Due to $N = \lceil M/K \rceil$ and the constraint in (5), there are at most K scheduled UEs in each group and K is constrained by

$$K_I = \max \left\{ 1, \left\lceil \frac{M}{N_{II}} \right\rceil \right\} \leq K \stackrel{(a)}{\leq} \min \left\{ L, \left\lceil \frac{M}{N_I} \right\rceil \right\} = K_{II}, \quad (6)$$

where step (a) in (6) is because $K \leq L$ and reflects the condition for exploiting spatial diversity and multiplexing gains through FAP CoMP [4]. We denote the k th scheduled UE in the n th group as $UE_{n,k}$, $\forall n \in [1, N]$ and $\forall k \in [1, K]$. Under constraint (6), the bandwidth allocated to each UE is $B(K) = \lfloor B^{\text{tot}}/(B_0 \lceil M/K \rceil) \rfloor B_0$.

Based on the aforementioned unified bandwidth allocation, UEs transmit signals that are received by all FAPs. Then, all FAPs forward the received signals to the CP for centralized signal processing, which includes CSI estimation based on the minimum mean-square error estimation method with orthogonal pilots and data detection based on zero-forcing (ZF) detection method under imperfect CSI [4]. Centralized signal processing is implemented at every time slot with duration $T_S = T_0$, where T_0 is the greatest common divisor across diverse D_{\max}^s and $T_C(v_r)$. One $T_C(v_r)$ contains $N_s = T_C(v_r)/T_S$ time slots and T_S comprises $N_f = T_S/T_f$ frames. To ensure accurate CSI estimation under service burstiness and diverse delay constraints, all UEs transmit pilots in each frame. If no service arrives, the data part of the frame is left empty, while pilot transmission is sustained. Thus, the pilot length ξ for accurate CSI estimation is constrained by [5]

$$K \leq \xi = B(K) N_f T_f^{(c)} \leq \xi_{\max} = B(K) N_f T_f - 1, \quad (7)$$

where ξ_{\max} is the maximum pilot length; $B(K) N_f T_f$ are the time-frequency resources for each service within T_S .

Based on [4], $g_{i,n,l,k}$, $\beta_{i,n,l,k}$, and $\psi_{i,n,l,k}$ denote the channel, the path loss, and the small-scale and shadowed fading from $UE_{n,k}$ to the l th FAP during time slot i , respectively; $\rho_p(K, \xi) = \rho(K)\xi$ is the pilot sequence power; $\rho(K) = \vartheta p_t/(B(K)\mathcal{N})$ and p_t are the transmit signal-to-noise ratio (SNR) and transmit power of each UE, respectively; \mathcal{N} is the noise power spectral density of the additive white Gaussian noise; $\vartheta \in (0, 1)$ is the SNR loss due to wireless fronthaul.

Lemma 2: Under the URA and the worst-case scenario with $d = \tilde{d}$, the LB on post-processing SNR of $UE_{n,k}$ in FAP CoMP-enabled AHetNets during time slot i can be given by

$$\hat{\gamma}_{i,n,k}^{\text{ZF, LB}}(K, \xi) = \hat{\rho}(K, \xi) \tilde{\beta} \sum_{l=1}^{L-K+1} |\hat{\psi}_{i,n,l,k}|^2, \quad (8)$$

where $\hat{\rho}(K, \xi) = \rho(K)/(K/\xi + 1)$; $\tilde{\beta} = \beta(\tilde{d})$ is the path loss under the worst-case scenario; $\hat{\psi}_{i,n,l,k} = \psi_{i,n,l,k} - \hat{w}_{i,n,l,k}$ is the estimated small-scale and shadowed fading

$$\eta_{\text{LB}}^{\text{H}}(U, K, \xi) = \mathbb{P}_{\psi} \left(\hat{\gamma}_{i,n,k}^{\text{ZF,LB}}(K, \xi) \geq \max \{ \gamma_{\text{th}}^{\zeta}((D_{\text{max}}^{\text{q},\zeta})_{u_{\text{I}}}, U, K, \xi), \forall u_{\text{I}} \in [1, U_{\text{I}}] \} \right) \times \prod_{u_{\text{II}}=1}^{U_{\text{II}}} \prod_{j=1}^{N_{\text{C}}} \left((D_{\text{max}}^{\text{s},v_{\text{r}}})_{u_{\text{II}}} \right) \mathbb{P}_{\psi} \left\{ \hat{\gamma}_{i+(j-1)N_{\text{s}},n,k}^{\text{ZF,LB}}(K, \xi) \geq \gamma_{\text{th}}^{\zeta}((D_{\text{max}}^{\text{q},\zeta})_{u_{\text{II}}}, U, K, \xi) \right\}, \zeta \in \{\text{LS, MS}\}. \quad (11)$$

from $UE_{n,k}$ to the l th FAP during time slot i ; $\hat{w}_{i,n,l,k} \sim \mathcal{CN}(0, 1/(\rho_{\text{p}}(K, \xi)\tilde{\beta} + 1))$ denotes the channel estimation error of $\psi_{i,n,l,k}$ under the worst-case scenario.

Proof: By substituting $\beta_{i,n,l,k} = \beta(\tilde{d})$ into the LB on post-processing SNR in [4], (8) can be obtained. \square

IV. NA ANALYSIS AND ENHANCEMENT

A. NA Analysis

From Section III-A, the delay constraints $D_{\text{max}}^{\text{s}}$ can be equivalent to the queueing delay constraints due to $D_{\text{max}}^{\text{q},\zeta} \triangleq D_{\text{max}}^{\text{s}} - D^{\text{u}}$. Thus, we consider utilizing effective bandwidth (EB) to analyze the LB on NA, since EB is a principal tool for representing queueing delay constraints [4]. Specifically, EB is defined as the minimal constant service rate that is required to satisfy $(D_{\text{max}}^{\text{q},\zeta}, \varepsilon_{\text{max}}^{\text{q},\zeta})$ for a stochastic arrival process, where $\varepsilon_{\text{max}}^{\text{q},\zeta}$ is the requirement of queueing delay violation probability. For stochastic arrival process $a^{\zeta}(t)$ (in bits/s), the formal definition of EB E_{B}^{ζ} (in packets/slot) is given by [14]

$$E_{\text{B}}^{\zeta}(D_{\text{max}}^{\text{q},\zeta}) = \lim_{t \rightarrow \infty} \frac{T_{\text{S}}}{\varpi^{\zeta} \Theta^{\zeta} t} \ln \mathbb{E}_{a^{\zeta}} \left[\exp \left(\Theta^{\zeta} \int_0^t a^{\zeta}(x) dx \right) \right], \quad (9)$$

where $\varpi^{\zeta}, \zeta \in \{\text{LS, MS}\}$ are the packet sizes (in bits) of the REC services under LSDC and MSDC, respectively; Θ^{ζ} is the QoS exponent that satisfies

$$\mathbb{P}_{a^{\zeta}}(D^{\text{q},\zeta} \geq D_{\text{max}}^{\text{q},\zeta}) \approx \exp(-\Theta^{\zeta} E_{\text{B}}^{\zeta} D_{\text{max}}^{\text{q},\zeta}) = \varepsilon^{\text{q},\zeta}, \quad (10)$$

where $\varepsilon^{\text{q},\zeta}$ is the queueing delay violation probability. If the service rate R^{ζ} is not less than E_{B}^{ζ} , then $(D_{\text{max}}^{\text{q},\zeta}, \varepsilon_{\text{max}}^{\text{q},\zeta})$ can be satisfied [4], [14], i.e., $(D^{\text{q},\zeta} \leq D_{\text{max}}^{\text{q},\zeta}, \varepsilon^{\text{q},\zeta} \leq \varepsilon_{\text{max}}^{\text{q},\zeta})$.

Hence, based on EB and Lemmas 1 ~ 2, we derive the expression for the LB on NA of AHetNets in Proposition 1, and analyze the impact of heterogeneity on the LB in Result 1. Especially, the degree of heterogeneity U is characterized by the number of delay constraints and mobility compositions. Under a composition $(D_{\text{max}}^{\text{s}}, v_{\text{r}})$, the number of coherence intervals is $N_{\text{C}}(D_{\text{max}}^{\text{s}}, v_{\text{r}}) = \lceil D_{\text{max}}^{\text{s}}/T_{\text{C}}(v_{\text{r}}) \rceil$. As mentioned in Section III-C, T_{S} is the greatest common divisor across diverse $D_{\text{max}}^{\text{s}}$ and $T_{\text{C}}(v_{\text{r}})$. Thus, T_{S} and N_{f} are functions of U , where $T_{\text{S}}(U)$ and $N_{\text{f}}(U)$ will reduce as U increases due to more diverse delay constraints and UE mobility.

Proposition 1: The LB on NA of FAP CoMP-enabled AHetNets with heterogeneity that stems from diverse delay constraints and UE mobility is expressed in (11) at the top of the page. Achieving $(\eta_{\text{LB}}^{\text{H}} \geq \eta_{\text{max}}, \eta_{\text{max}} \rightarrow 1)$ implies that the target NA (i.e., $\eta_{\text{max}} \rightarrow 1$) is achieved. In (11), $(D_{\text{max}}^{\text{q},\zeta})_{u_{\text{I}}}, \forall u_{\text{I}} \in [1, U_{\text{I}}]$ and $(D_{\text{max}}^{\text{q},\zeta})_{u_{\text{II}}}, \forall u_{\text{II}} \in [1, U_{\text{II}}]$ denote the queueing delay constraints when $D_{\text{max}}^{\text{s}} \leq T_{\text{C}}$ and $D_{\text{max}}^{\text{s}} > T_{\text{C}}$, respectively; $(D_{\text{max}}^{\text{s},v_{\text{r}}})_{u_{\text{II}}}$ denote the delay constraints and UE mobility compositions under $D_{\text{max}}^{\text{s}} > T_{\text{C}}$. Moreover, $U = U_{\text{I}} + U_{\text{II}}$, where U_{I} and U_{II} are the numbers of delay constraints and UE mobility compositions under $D_{\text{max}}^{\text{s}} \leq T_{\text{C}}$ and $D_{\text{max}}^{\text{s}} > T_{\text{C}}$, respectively. Finally, $\gamma_{\text{th}}^{\zeta}(D_{\text{max}}^{\text{q},\zeta}, U, K, \xi)$

are required thresholds of post-processing SNR for satisfying $(D_{\text{max}}^{\text{s}}, \varepsilon_{\text{max}}^{\text{s}})$, which are expressed as

$$\gamma_{\text{th}}^{\text{LS}}(\mathcal{P}^{\text{LS}}) = \phi \exp \left(\frac{\varpi^{\text{LS}} E_{\text{B}}^{\text{LS}}(D_{\text{max}}^{\text{q,LS}}) \ln 2}{B(K) N_{\text{f}}(U) T_{\text{f}} - \xi} \right), \quad (12)$$

$$\gamma_{\text{th}}^{\text{MS}}(\mathcal{P}^{\text{MS}}) = \exp \left(\frac{\varpi^{\text{MS}} E_{\text{B}}^{\text{MS}}(D_{\text{max}}^{\text{q,MS}}) \ln 2}{B(K) N_{\text{f}}(U) T_{\text{f}} - \xi} + \frac{f_{\text{Q}}^{-1}(\varepsilon_{\text{max}}^{\text{u,c}})}{\sqrt{B(K) T_{\text{f}}^{(\text{d})}}} \right) - 1, \quad (13)$$

where $\phi > 1$ is the SNR loss due to the finite blocklength [10]; $\mathcal{P}^{\zeta} = \{D_{\text{max}}^{\text{q},\zeta}, U, K, \xi\}$, $\zeta \in \{\text{LS, MS}\}$; $\varepsilon_{\text{max}}^{\text{u,c}} = \varepsilon_{\text{max}}^{\text{MS}} - \varepsilon_{\text{max}}^{\text{q,MS}}$ is the requirement of decoding error probability.

Proof: See Appendix A. \square

Result 1: From (11), $\eta_{\text{LB}}^{\text{H}}$ decreases under extended heterogeneity, even when the heterogeneity stems from additional REC services under LSDC or from UEs with lower mobility. The reason is that $\gamma_{\text{th}}^{\zeta}(\mathcal{P}^{\zeta})$ in (12) and (13) increase with extended heterogeneity, which is due to the reduction in the time-frequency resources $B(K) N_{\text{f}}(U) T_{\text{f}}$ for each service with increased U .

B. NA Enhancement

Based on the insights in Result 1, it is necessary to improve resource efficiency to enhance the LB on NA for mitigating the impact of heterogeneity. Thus, we analytically obtain Property 1 and formulate the optimization problem in this part.

Property 1: Since $B(K) = \lfloor B^{\text{tot}}/(B_0 \lceil M/K \rceil) \rfloor B_0$, the time-frequency resources of each service can be increased under a larger K . However, $\hat{\gamma}_{i,n,k}^{\text{ZF,LB}}(K, \xi)$ in (8) decreases with larger K due to increased interference and reduced spatial diversity, degrading $\eta_{\text{LB}}^{\text{H}}$. Moreover, a higher ξ may be required due to $\xi \geq K$ in (7), which shortens the time-frequency resources for data transmission, i.e., $B(K) N_{\text{f}}(U) T_{\text{f}} - \xi$. Consequently, $\gamma_{\text{th}}^{\zeta}(\mathcal{P}^{\zeta})$ in (12) and (13) increase, further degrading $\eta_{\text{LB}}^{\text{H}}$. Therefore, K and ξ should be jointly optimized to improve spatial, frequency, and temporal resource efficiency.

Based on Property 1, we formulate the following optimization problem to jointly optimize K and ξ .

$$\max_{K, \xi} \eta_{\text{LB}}^{\text{H}}(U, K, \xi) \quad (14)$$

s.t. (5), (6), (7).

The optimal values of K and ξ , denoted by K^* and ξ^* , respectively, for the problem (14), can be obtained using the exhaustive search method. The complexity of this method is $\mathcal{O}((\xi_{\text{max}} + 1)(K_{\text{II}} - K_{\text{I}} + 1) - 0.5(K_{\text{II}} + K_{\text{I}})(K_{\text{II}} - K_{\text{I}} + 1))$.

V. SIMULATION AND NUMERICAL RESULTS

In this section, we validate our analysis and results by presenting numerical simulations through 10^{10} Monte-Carlo trials. For our simulations, we consider a disaster area with a radius of $W_{\text{D}} = 3,000$ m, where $M = 1,000$ UEs are all

TABLE I
SOURCES OF HETEROGENEITY

Sources	S ₁	S ₂	S ₃	S ₄
D_{\max}^{LS} (ms)	55:5:105	55	55:5:105	55:-5:5
v_r (m/s)	30	30:-2:10	30:-2:10	30:2:50

TABLE II
SIMULATION PARAMETERS [3], [4], [11]

Parameter	Value
Duration of each frame T_f (equals to TTI)	0.1 ms
Orthogonal subcarrier spacing B_0	15 KHz
Carrier frequency f_c	2 GHz
Sampling time t_s	66.66 μ s
Channel coherence bandwidth B_C	0.5 MHz
Noise power spectral density \mathcal{N}	-174 dBm/Hz
Transmit power ρ_t	5 dBm
Packet size $\varpi^{\text{LS}}/\varpi^{\text{MS}}$	1000/160 bits

activated. The FAP flight altitude is set as $h_F = 200$ m. The AUE flight altitude range is set as $\mathcal{H} = [100, 400]$ m. The κ - μ shadowed fading parameters are set as $\kappa \rightarrow 0$, $\mu = 3$, and $m \rightarrow \infty$ for characterizing the Nakagami- m fading, which is generally used in aerial networks [4]. The SNR losses due to wireless fronthaul and finite blocklength are set as $\vartheta = 0.5$ and $\phi = 1.5$, respectively. The requirement of uOPL probability is set as $\varepsilon_{\max}^{\text{c}} = 10^{-5}$, $\varsigma \in \{\text{LS}, \text{MS}\}$, where $\varepsilon_{\max}^{\text{u,c}} = \varepsilon_{\max}^{\text{q,MS}} = \frac{1}{2}\varepsilon_{\max}^{\text{MS}}$ and $\varepsilon_{\max}^{\text{q,LS}} = \varepsilon_{\max}^{\text{LS}}$. In disaster emergency scenarios, the total delay bound in uplink RECs under MSDC is $D_{\max}^{\text{MS}} = 0.5$ ms, and the relative velocity is $v_r = 30$ (m/s) [4]. For uplink RECs under LSDC, there are four groups of total delay bound D_{\max}^{LS} and relative velocity v_r , which act as four sources of heterogeneity. The details of the four sources are shown in Table I. The degree of heterogeneity $U = Z$, $Z \geq 2$ indicates that the scenario contains RECs under MSDC and LSDC with $(D_{\max}^{\text{LS}}(1), v_r(1)) \sim (D_{\max}^{\text{LS}}(Z-1), v_r(Z-1))$; $U = 1$ refers to the scenario that contains RECs under MSDC. The target NA is set as $\eta_{\max} = 0.98$. The total bandwidth is $B^{\text{tot}} = 150$ MHz. We consider the service stochastic arrival process as the Poisson process, where $\theta^{\text{c}} = \sigma_{\text{c}}^2$, $\lambda^{\text{LS}} = 500$ packets/s, and $\lambda^{\text{MS}} = 20$ packets/s. The EB (in packets/slot) for a Poisson arrival process is $E_B^{\text{c}} = \frac{N_f T_f \ln(1/\varepsilon_{\max}^{\text{q,MS}})}{D_{\max}^{\text{q,S}} \ln[T_f \ln(1/\varepsilon_{\max}^{\text{q,S}})] / (\theta^{\text{c}} D_{\max}^{\text{q,S}}) + 1}$ [4]. The other parameters are listed in Table II.

Figure 1 shows the impact of different sources of heterogeneity on $\eta_{\text{LB}}^{\text{H}}$. The results indicate that as the degree of heterogeneity U increases, $\eta_{\text{LB}}^{\text{H}}$ experiences significant degradation, even when the heterogeneity stems from additional REC services under LSDC or from UEs with lower mobility. Notably, when heterogeneity is driven by both additional REC services under LSDC and UEs with higher mobility, as in the source of S₄, the degradation in $\eta_{\text{LB}}^{\text{H}}$ becomes super-linear. These findings validate *Result 1*, confirming the pronounced sensitivity of $\eta_{\text{LB}}^{\text{H}}$ to extended heterogeneity in AHetNets.

Figure 2 shows the impact of heterogeneity—caused by S₄ on $\eta_{\text{LB}}^{\text{H}}$ under various resource allocation policies. These policies include: existing (i) fixed values for both K and ξ , (ii) optimization of K only, (iii) optimization of ξ only, and our proposed (iv) joint optimization of K and ξ . In the figure, the legend “Baseline” corresponds to the policy that $K = 6$ and ξ is fixed, specifically with $T_f^{(\text{c})} = 0.05$ ms. The legend

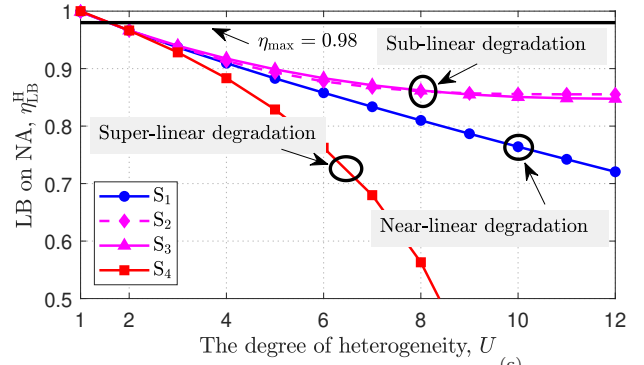


Fig. 1. LB on NA vs. U with $L = 15$, $K = 6$, and $T_f^{(\text{c})} = 0.05$ ms.

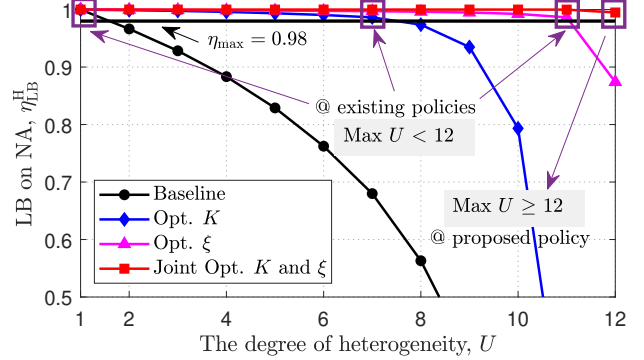


Fig. 2. LB on NA vs. U under different K and ξ with $L = 15$.

“Opt. K ” represents the policy that only K is optimized, while ξ remains fixed. Similarly, “Opt. ξ ” refers to optimizing ξ with K fixed at 6. The legend “Joint Opt. K and ξ ” indicates the policy that both K and ξ are jointly optimized. Besides, “Max U ” is the maximum U , where $(\eta_{\text{LB}}^{\text{H}} \geq \eta_{\max}, \eta_{\max} \rightarrow 1)$ can be achieved. Compared to existing policies, the joint optimization of K and ξ significantly enhances the ability to achieve $(\eta_{\text{LB}}^{\text{H}} \geq \eta_{\max}, \eta_{\max} \rightarrow 1)$ in AHetNets, especially under increased heterogeneity. This demonstrates that the proposed joint optimization policy effectively mitigates NA degradation caused by extended heterogeneity, thereby validating the effectiveness of *Property 1* and the optimization problem in (14) for achieving the target NA in AHetNets.

VI. CONCLUSION

We investigated the NA of FAP CoMP-enabled AHetNets for delay-constrained REC services to UEs with varying mobility. To address resource allocation conflicts from heterogeneity in delay constraints and mobility, we employed a URA scheme. We derived expressions for the LB on NA, revealing that extended heterogeneity significantly degrades it. To mitigate this, we jointly optimized the number of UEs sharing time-frequency resources (K) and the pilot length (ξ), improving the LB. Simulations confirmed that target NA levels are achievable even under greater heterogeneity through joint optimization of K and ξ .

APPENDIX A

PROOF OF PROPOSITION 1

Under diverse D_{\max}^{S} and T_C , it is likely to observe $D_{\max}^{\text{S}} \leq T_C$ and $D_{\max}^{\text{S}} > T_C$, $\varsigma \in \{\text{LS}, \text{MS}\}$, which result in quasi-static and time-varying channels, respectively [4], [11].

1) NA when $D_{\max}^{\text{LS}} > T_C$: For delay-sensitive services, even if the delay constraints are less stringent, the blocklength of channel coding is finite [10]. Then, with a specific SNR γ , the achievable service rate (packets/slot) under LSDC is [10]

$$R^{\text{LS}} = \frac{BN_f T_f^{(d)}}{\varpi^{\text{LS}} \ln 2} C\left(\frac{\gamma}{\phi}\right), \quad (15)$$

where $C(\gamma) = \ln(1 + \gamma)$ is Shannon's capacity in the infinite blocklength regime; $BT_f^{(d)}$ is the blocklength of channel coding during each frame (in the number of channel uses); $BN_f T_f^{(d)} = BN_f T_f - \xi$ is the time-frequency resources for data transmission of each service during each time slot.

From [10], packet loss comes from queueing delay violations for the services under LSDC. Then, the QoS requirement $(D_{\max}^{\text{LS}}, \varepsilon_{\max}^{\text{LS}})$ for ensuring REC services under LSDC can be equated to $(D_{\max}^{\text{q,LS}}, \varepsilon_{\max}^{\text{q,LS}})$. In time-varying channels, $\hat{\gamma}_{i,n,k}^{\text{ZF,LS}} = \hat{\gamma}_{i',n,k}^{\text{ZF,LS}}, \forall i, i' \in [0, I], |i - i'| \leq N_s$ and $\hat{\gamma}_{i,n,k}^{\text{ZF,LS}} = \hat{\gamma}_{i+N_s,n,k}^{\text{ZF,LS}} \cup \hat{\gamma}_{i,n,k}^{\text{ZF,LS}} \neq \hat{\gamma}_{i+N_s,n,k}^{\text{ZF,LS}}$. Consequently, R^{LS} varies across different T_C within D_{\max}^{LS} and remains constant during each T_C . Then, $(D_{\max}^{\text{q,LS}}, \varepsilon_{\max}^{\text{q,LS}})$ can be satisfied if $R^{\text{LS}} \geq E_B^{\text{LS}}$ can be assured during each T_C within D_{\max}^{LS} . Thus, by substituting $R^{\text{LS}} = E_B^{\text{LS}}$ into (15), we get the required threshold of post-processing SNR $\gamma_{\text{th}}^{\text{LS}}$ for satisfying $(D_{\max}^{\text{LS}}, \varepsilon_{\max}^{\text{LS}})$, which is given in (12). Based on Lemma 1, the LB on NA for REC services under LSDC with identical $(D_{\max}^{\text{LS}}, \varepsilon_{\max}^{\text{LS}})$ of UEs with same mobility when $D_{\max}^{\text{LS}} > T_C$ can be given by

$$\hat{\eta}_{\text{LB}}^{\text{LS}} = \prod_{j=1}^{N_C} \mathbb{P}_{\psi}(\hat{\gamma}_{i+(j-1)N_s,n,k}^{\text{ZF,LS}} \geq \gamma_{\text{th}}^{\text{LS}}). \quad (16)$$

2) NA when $D_{\max}^{\text{MS}} \leq T_C$: When the delay constraints are more stringent, the blocklength of channel coding is significantly shorter [10]. As a result, decoding errors cannot be ignored under MSDC. According to finite blocklength information theory, the achievable service rate R^{MS} (packets/slot) of UE with a specific SNR γ and a given decoding error probability $\varepsilon^{\text{u,c}}$ can be given by [10]

$$R^{\text{MS}} = \frac{BN_f T_f - \xi}{\varpi^{\text{MS}} \ln 2} \left[C(\gamma) - \sqrt{\frac{V(\gamma)}{BT_f^{(d)}}} f_{Q^{-1}}(\varepsilon^{\text{u,c}}) \right], \quad (17)$$

where $V(\gamma) = 1 - \frac{1}{(1+\gamma)^2} \leq 1$ is the channel dispersion.

From [4], [10], packet loss comes from decoding errors and queueing delay violations for services under MSDC. According to [4], by integrating the decoding error probability $\varepsilon^{\text{u,c}}$ and the queueing delay violation probability $\varepsilon^{\text{q,MS}}$, the uOPL probability is given by $\varepsilon_{\max}^{\text{MS}} \leq \varepsilon^{\text{u,c}} + \varepsilon^{\text{q,MS}}$. For QoS requirements $(D_{\max}^{\text{MS}}, \varepsilon_{\max}^{\text{MS}})$, $\varepsilon_{\max}^{\text{MS}}$ can be divided into $\varepsilon_{\max}^{\text{u,c}}$ and $\varepsilon_{\max}^{\text{q,MS}}$ under the delay constraints D_{\max}^{MS} , i.e., $\varepsilon_{\max}^{\text{MS}} = \varepsilon_{\max}^{\text{u,c}} + \varepsilon_{\max}^{\text{q,MS}}$, where $\varepsilon_{\max}^{\text{u,c}}$ is the requirement of $\varepsilon^{\text{u,c}}$. In quasi-static channels, R^{MS} is constant within D_{\max}^{MS} [4]. By substituting $R^{\text{MS}} = E_B^{\text{MS}}$, $\varepsilon^{\text{u,c}} = \varepsilon_{\max}^{\text{u,c}}$, and $V(\gamma) = 1$ into (17), we can obtain the required threshold of post-processing SNR $\gamma_{\text{th}}^{\text{MS}}$ for satisfying $(D_{\max}^{\text{MS}}, \varepsilon_{\max}^{\text{MS}})$, which is given in (13).

Based on Lemma 1, the LB on NA for REC services under MSDC with identical $(D_{\max}^{\text{MS}}, \varepsilon_{\max}^{\text{MS}})$ of UEs with same mobility when $D_{\max}^{\text{MS}} \leq T_C$ can be expressed as

$$\hat{\eta}_{\text{LB}}^{\text{MS}} = \mathbb{P}_{\psi}(\hat{\gamma}_{i,n,k}^{\text{ZF,LS}} \geq \gamma_{\text{th}}^{\text{MS}}). \quad (18)$$

3) NA when $D_{\max}^{\text{LS}} \leq T_C$: Based on (12) and (18), the LB on NA for REC services under LSDC with identical

$(D_{\max}^{\text{LS}}, \varepsilon_{\max}^{\text{LS}})$ of UEs with same mobility, when $D_{\max}^{\text{LS}} \leq T_C$, can be given by

$$\hat{\eta}_{\text{LB}}^{\text{LS}} = \mathbb{P}_{\psi}(\hat{\gamma}_{i,n,k}^{\text{ZF,LS}} \geq \gamma_{\text{th}}^{\text{LS}}). \quad (19)$$

4) NA under $D_{\max}^{\text{MS}} > T_C$: Based on (13) and (16), the LB on NA for REC services under MSDC with identical $(D_{\max}^{\text{MS}}, \varepsilon_{\max}^{\text{MS}})$ of UEs with same mobility, when $D_{\max}^{\text{MS}} > T_C$, can be given by

$$\hat{\eta}_{\text{LB}}^{\text{MS}} = \prod_{j=1}^{N_C} \mathbb{P}_{\psi}(\hat{\gamma}_{i+(j-1)N_s,n,k}^{\text{ZF,LS}} \geq \gamma_{\text{th}}^{\text{MS}}). \quad (20)$$

Since $\hat{\eta}_{\text{LB}}^{\text{MS}}, \varsigma \in \{\text{LS}, \text{MS}\}$, in (18) and (19) depend only on $\gamma_{\text{th}}^{\text{MS}}$, ensuring the REC with a higher $\gamma_{\text{th}}^{\text{MS}}$ automatically ensures the REC with a lower $\gamma_{\text{th}}^{\text{MS}}$. Ensuring REC when $D_{\max}^{\text{MS}} > T_C$ is independent of the case when $D_{\max}^{\text{MS}} \leq T_C$, since $\hat{\eta}_{\text{LB}}^{\text{MS}}$ in (16) and (20) depends on both $\gamma_{\text{th}}^{\text{MS}}$ and N_C . Moreover, when $D_{\max}^{\text{MS}} > T_C$, REC under different delay constraints shows weak coupling across UEs with varying mobility. Specifically, ensuring REC with larger $\gamma_{\text{th}}^{\text{MS}}$ or N_C does not guarantee it for smaller values, even though $\hat{\eta}_{\text{LB}}^{\text{MS}}$ increases as $\gamma_{\text{th}}^{\text{MS}}$ or N_C decreases. This is because a smaller N_C , due to stringent D_{\max}^{MS} , is accompanied by a larger $\gamma_{\text{th}}^{\text{MS}}$. Finally, by combining NAs across delay constraints and mobility levels, we derive a LB on overall NA valid for both $D_{\max}^{\text{MS}} \leq T_C$ and $D_{\max}^{\text{MS}} > T_C$. Based on this, (11) follows, completing the proof.

REFERENCES

- [1] N.-N. Dao *et al.*, "Survey on aerial radio access networks: Toward a comprehensive 6G access infrastructure," *IEEE Commun. Surveys Tuts.*, vol. 23, no. 2, pp. 1193–1225, 2nd Quarter 2021.
- [2] Z. Yao, W. Cheng, W. Zhang, T. Zhang, and H. Zhang, "The rise of UAV fleet technologies for emergency wireless communications in harsh environments," *IEEE Netw.*, vol. 36, no. 4, pp. 28–37, Jul. 2022.
- [3] Z. Liu, K. Li, Y. Wang, and P. Zhu, "Mixed traffic scheduling with latency and jitter analysis in URLLC industrial automation," *IEEE Internet Things J.*, vol. 12, no. 12, pp. 18 820–18 835, Jun. 2025.
- [4] J. Liu *et al.*, "Towards reliable communications with delay requirement in aerial disaster emergency networks via coordinated multi-point," *IEEE Trans. Commun.*, vol. 73, no. 10, pp. 8781–8796, Oct. 2025.
- [5] M. Mohammadi, Z. Mobini, H. Q. Ngo, and M. Matthaiou, "Next-generation multiple access with cell-free massive MIMO," *Proc. IEEE*, vol. 112, no. 9, pp. 1372–1420, Sept. 2024.
- [6] M. Elwekeil *et al.*, "Power control in cell-free massive MIMO networks for UAVs URLLC under the finite blocklength regime," *IEEE Trans. Commun.*, vol. 71, no. 2, pp. 1126–1140, Feb 2023.
- [7] L. Liu, S. Wu, and Y. Ma, "Resource allocation in cell-free massive MIMO with the coexistence of eMBB and URLLC," *IEEE Trans. Veh. Technol.*, vol. 74, no. 10, pp. 16 039–16 054, Oct. 2025.
- [8] X. Zhang *et al.*, "Multi-agent deep reinforcement learning-based uplink power control in cell-free massive MIMO with mobile users," *IEEE Trans. Veh. Technol.*, pp. 1–16, 2025 (Early Access).
- [9] M. S. Abbas, Z. Mobini, H. Q. Ngo, H. Shin, and M. Matthaiou, "Joint AP selection and power allocation for unicast-multicast cell-free massive MIMO," *IEEE Internet Things J.*, vol. 12, no. 22, pp. 47 135–47 150, Nov. 2025.
- [10] R. Dong *et al.*, "Deep learning for radio resource allocation with diverse quality-of-service requirements in 5G," *IEEE Trans. Wireless Commun.*, vol. 20, no. 4, pp. 2309–2324, Apr. 2021.
- [11] S. Elhoushy and W. Hamouda, "Limiting Doppler shift effect on cell-free massive MIMO systems: A stochastic geometry approach," *IEEE Trans. Wireless Commun.*, vol. 20, no. 9, pp. 5656–5671, Sept. 2021.
- [12] *Service Requirements for the 5G System*, Technical Specification (TS) 22.261, 3rd Generation Partnership Project, Jun. 2022.
- [13] M. A. Imran *et al.*, "Exploring the boundaries of connected systems: Communications for hard-to-reach areas and extreme conditions," *Proc. IEEE*, vol. 112, no. 7, pp. 912–945, Jul. 2024.
- [14] C. She *et al.*, "A tutorial on ultrareliable and low-latency communications in 6G: Integrating domain knowledge into deep learning," *Proc. IEEE*, vol. 109, no. 3, pp. 204–246, Mar. 2021.